

Bond and ductility: a theoretical study on the impact of construction details – part 1: basic considerations

Daia Zwicky*

University of Applied Sciences Western Switzerland, College of Engineering and Architecture of Fribourg, CH-1705 Fribourg, Switzerland

(Received November 17, 2012, Revised December 28, 2012, Accepted February 7, 2013)

Abstract. The applicability of limit analysis methods in design and assessment of concrete structures generally requires a certain plastic deformation capacity. The latter is primarily provided by the ductility of the reinforcement, being additionally affected by the bond properties between reinforcing steel and concrete since they provoke strain localization in the reinforcement at cracks. The bond strength of reinforcing bars is not only governed by concrete quality, but also by construction details such as bar ribbing, bar spacing or concrete cover thickness. For new concrete structures, a potentially unfavorable impact on bond strength can easily be anticipated through appropriate code rules on construction details. In existing structures, these requirements may not be necessarily satisfied, consequently requiring additional considerations. This two-part paper investigates in a theoretical study the impacts of the most frequently encountered construction details which may not satisfy design code requirements on bond strength, steel strain localization and plastic deformation capacity of cracked structural concrete. The first part introduces basic considerations on bond, strain localization and plastic deformation capacity as well as the fundamentals of the Tension Chord Model underlying the further investigations. It also analyzes the impacts of the hardening behavior of reinforcing steel and concrete quality. The second part discusses the impacts of construction details (bar ribbing, bar spacing, and concrete cover thickness) and of additional structure-specific features such as bar diameter and crack spacing.

Keywords: analytical approach; assessment; anchorage; bond; codes; constitutive models; detailing; plasticity; reinforcing bars

1. Introduction

The refined verification of structural safety of concrete structures may require the application of more sophisticated analysis tools and verification approaches. Applying limit analysis tools, i.e. analysis based on the theory of plasticity (e.g. Nielsen and Hoang 2010), allows a more realistic estimation of ultimate bearing capacity of structural concrete.

Usually, the application of the so-called lower-bound method is preferred, providing a conservative estimate of ultimate load. It targets to find a state of stress that satisfies equilibrium and static boundary conditions without surpassing the available structural resistances in any point

*Corresponding author, Professor, E-mail: daia.zwicky@hefr.ch

of the structure but it usually disregards compatibility conditions. Attaining such a statically admissible stress state may be associated with pronounced plastic redistribution of internal forces, e.g. rotation in plastic hinges or inclination changes of compression fields in girder webs associated to plastic deformations of the shear reinforcement. If a structure does not provide sufficient plastic deformation capacity (i.e., ductility), the ultimate load according to the lower-bound method cannot be attained and the load bearing capacity is overestimated.

For new concrete structures, the necessary plastic deformation capacity that is implicitly or explicitly considered can be ensured rather easily through appropriate choice of construction materials, by providing the structure with a minimum reinforcement and by appropriate construction details. Since these requirements may not be necessarily fulfilled for existing structures, plastic deformation capacities must eventually be checked explicitly, in order to determine correctly ultimate load bearing capacities, thereby (eventually) avoiding expensive strengthening measures.

The ductility of structural concrete may be considerably affected by construction details. This is due to their impact on bond properties between reinforcement and concrete which, in turn, have an impact on plastic deformation capacity. Therefore, more detailed investigations should be performed if construction details and other structure-specific features do not satisfy actual design code requirements.

2. Basic considerations

2.1 Reinforcement details and bond strength

The bond strength of reinforcing bars depends on a large number of construction details and other structure-specific features (fib 2000):

- Ribbing of reinforcing bars, i.e., geometrical form and spacing of ribs
- Bar spacing or clear space between bars, respectively
- Number of bar layers or of bundled bars
- Position of reinforcing bars during concreting or concrete quality around the bars, respectively
- Thickness of concrete cover
- State of strain in the reinforcing bar, i.e. elastic or plastic strain
- Steel corrosion
- Lateral pressure and confinement
- Service temperature
- Load time-history, etc.

Many of these influences on bond strength can easily be anticipated in the design of new concrete structures through appropriate construction requirements in codes, providing presumed bond properties. In existing structures, however, construction details cannot be changed anymore; the assessment engineer thus needs a basis for treating the encountered circumstances. Providing a basis for associated examinations is essential since more and more projects in daily structural engineering practice deal with existing structures. Their share will further increase in the future, at least in well-developed countries where new infrastructure is already built to a large extent.

More detailed information on how to assess the impact of the most frequently encountered construction details, i.e. concrete cover thickness, bar ribbing, and bar spacing, on bond strength has therefore been integrated in the recent Swiss code SIA 269/2 (2011) on existing concrete

structures. The associated code chapter, among others, was developed under the guidance of the author and is outlined in more detail hereafter. More information on the complete code series SIA 269 on existing structures can be found in Brühwiler *et al.* (2012).

Issues related to bar layers, bundled bars, steel corrosion, lateral pressure, unusual temperature ranges and time-variant loading are not addressed in the following.

2.2 Plastic deformation capacity of structural concrete

Plastic deformation capacity of structural concrete is essentially provided by inelastic strains of the reinforcement. The latter are evidently only available if the steel is strained beyond yielding but does not rupture.

2.2.1 Rotation capacity of plastic hinges

For an approximate analysis, it may be assumed that plastic deformations in a flexural girder concentrate in point-shaped plastic hinges providing a maximum rotation angle θ_{pl} . Further assuming that plane sections remain plane, i.e., compatibility of strains, this angle can be estimated from the lower value provided by the following expressions (Sigrist and Marti 1994)

$$\theta_{pl}^{(s)} = \frac{d}{d-x} (\varepsilon_{smu} - \varepsilon_{smy}) = \frac{1}{1-\omega} (\varepsilon_{smu} - \varepsilon_{smy}) = \frac{1}{1-\omega} \Delta\varepsilon_{pl} \quad (1)$$

and

$$\theta_{pl}^{(c)} = d \left(\frac{\varepsilon_{cnu}}{x} - \frac{\varepsilon_{smy}}{d-x} \right) = \frac{\varepsilon_{cnu}}{\omega} - \frac{\varepsilon_{smy}}{1-\omega} \quad (2)$$

where d = effective depth of the reinforcement; x = plastic height of compression zone; ε_{smu} = average steel strain at attaining the ultimate strain ε_{su} ; ε_{smy} = average steel strain at attaining the yield strain ε_{sv} ; ω = mechanical reinforcement ratio, Eq. (3); $\Delta\varepsilon_{pl} = \varepsilon_{smu} - \varepsilon_{smy}$; and ε_{cnu} = nominal concrete crushing strain in the compression zone. The plastic height of the compression zone $x = \omega d$ is determined from

$$\omega = \frac{A_s f_{sy}}{bd f_{cu}} \quad (3)$$

where A_s = cross-section of longitudinal reinforcement; f_{sy} = yield strength of reinforcing steel; b = width of the compression zone and f_{cu} = uniaxial concrete compressive strength.

Eq. (1) represents the plastic rotation capacity provided by the reinforcement, assuming that the length of the plastic hinge zone corresponds to the effective depth d (which usually is a conservative assumption), and that the deformations of this plastic hinge zone concentrate in a point-shaped hinge. For a concrete girder with given reinforcement, geometry and material properties, the available plastic rotation capacity is thus governed by the difference $\Delta\varepsilon_{pl}$ of the average steel strains at rupture and at yielding, i.e., by the expression in brackets of Eq. (1).

Eq. (2) represents the rotation capacity of the plastic hinge if crushing of the concrete compression zone governs, often assumed at a nominal crushing strain of $\varepsilon_{cnu} = 3\%$ to 5% (Bachmann 1967, Sigrist 1995). This potential rupture criterion is not addressed here in detail.

For evaluating the impact of structure-specific features on bond, strain localization and ductility of structural concrete, the further analyses performed here therefore focus on $\Delta\varepsilon_{pl}$, thus assuming that the mechanical reinforcement ratio ω of the tension chord is constant. Note that applying Eqs.

(1) and (2) corresponds to a simplified approach; the available plastic deformation capacity usually cannot be analyzed separately from the required plastic deformation capacity since they are related through the static system, the load arrangement, and the necessary or assumed plastic redistribution of internal forces, respectively. It can also be shown (Sigrist 1995) that the required plastic deformation capacity depends on further parameters such as available mechanical reinforcement ratios in the governing girder sections, slenderness of the girder, geometrical properties of the cross-section, shear reinforcement ratio and effective compressive strength of the web concrete, ductility properties of the reinforcing steel, and bond properties between reinforcement and concrete.

2.2.2 Strain compatibility and steel strain localization in structural concrete

Strain compatibility in structural concrete only applies to average strains since cracks form at discrete distances. Average reinforcement strains are lower than the maximum strains at cracks due to the tension stiffening effect of the concrete between the cracks; this effect is also called (steel) strain localization (at cracks). While strain compatibility is expressed and valid for average strains, the higher steel strains at cracks have to be considered for assessing the exploitation of the mechanical properties of the reinforcement.

Strain localization is strongly affected by the bond properties between reinforcement and concrete and by the hardening behavior of the reinforcing steel (Alvarez 1998, Eligehausen and Mayer 2000, fib 2000, Mayer 2003). Therefore, the consideration of these two basic features is generally prescribed in SIA 269/2 (2011) for ductility assessment.

An efficient means for considering the difference in average steel strains and maximum strains at cracks in strain compatibility conditions is introducing a so-called strain localization factor or bond coefficient $\kappa_s = \varepsilon_{sm}/\varepsilon_{max}$ (Bachmann 1967, fib 2000), expressing the ratio of average steel strain ε_{sm} between two adjacent cracks to maximum steel strain ε_{max} at cracks. Such strain localization factors can be derived, for example, from the Tension Chord Model (Section 2.3). This allows the consideration of the exploitation of the ductility properties of the reinforcement at cracks when determining the available rotation capacity of a plastic hinge in terms of average strains, Eq. (1). A strain localization factor κ_s tending towards 1 corresponds to the limit cases of unbonded or rigidly bonded reinforcement resulting in infinitely small crack spacing. A strain localization factor κ_s tending towards 0 represents high concentration of steel strains at cracks or high tension stiffening, respectively.

2.2.3 Plastic deformations of reinforcing steel

In the case of hot-rolled reinforcing steel with a yield plateau, the yield strain ε_{sy} is simply derived from $\varepsilon_{sy} = f_{sy}/E_s$ with f_{sy} = yield strength and E_s = Young's modulus, leading to values of $\varepsilon_{sy} \approx 2.5\text{‰}$ for common reinforcing steel. Every steel strain at cracks above ε_{sy} implies plastic deformation.

For cold-worked reinforcing steel, no yield plateau is available. A nominal yield strength is usually defined at a residual strain of $\varepsilon_{s,pl} = 2\text{‰}$, being thus associated with a total yield strain of $\varepsilon_{sy} = f_{sy}/E_s + 2\text{‰} \approx 4.5\text{‰}$ for common reinforcing steel. However, this definition of ε_{sy} is debatable for the determination of plastic deformation capacity since the referred limit of residual strain, i.e., plastic strain, is of the same order of magnitude as the strain associated with the nominal yield strain. Plastic stress redistribution may start at a much lower stress level, usually after exceeding the proportional limit. The latter is habitually defined at a residual strain of 0.1‰ , thus being associated with a total strain of $\varepsilon_{sp} = f_{sy}/E_s + 0.1\text{‰} \approx 2.6\text{‰}$ for common reinforcing steel.

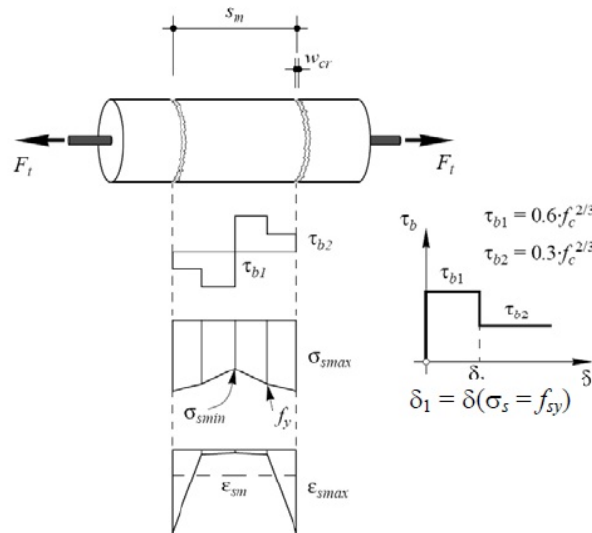


Fig. 1 Tension Chord Model (Sigrist 1995)

Hereafter, the impact of both options of defining the onset of plastic steel strains is analyzed.

2.3 Tension chord model

The bond model behind the directives in SIA 269/2 (2011) is the same as in the code SIA 262 (2003): the Tension Chord Model (Marti *et al.* 1998), Fig. 1.

This model was initially developed for studying the deformation capacity of flexural plastic hinges in reinforced concrete girders (Sigrist and Marti 1994, Sigrist 1995), simplifying the mechanical behavior of reinforcing steel by a bilinear constitutive law (Fig. A.1(a)). It was extended to the consideration of more realistic hardening behavior of reinforcing and prestressing steel (Alvarez 1998), Figs. A.1(b) and (c), and to the analysis of plane stress problems (Kaufmann 1998, Kaufmann and Marti 1998), i.e., analysis of wall elements and girder webs in shear. Finally, the model was also successfully applied to serviceability limit state problems, i.e., cracking behavior and crack width calculation, minimum reinforcement and tension stiffening effects (Marti *et al.* 1997, Kenel 2002, Burns 2011). Note that the Tension Chord Model mainly targets at determining overall deformation behavior of structural concrete. Furthermore, it should not be applied indiscriminately to fatigue problems or corroded concrete structures.

The fundamental hypothesis of the Tension Chord Model is the proposed bond-slip relationship: a two-stage, rigid-plastic bond-slip constitutive law where the decrease in bond stress takes place at reinforcement yielding (Fig. 1), motivated by experimental observations of considerable reductions in bond strength after attaining steel yielding (Shima *et al.* 1987, Engström 1992).

This assumption for the bond-slip relationship is particularly useful since it uncouples the bond stress from the slip of the reinforcing bar, i.e., the relative displacement between bar and surrounding concrete. The steel stress can thus be derived from equilibrium only without the need of integrating the differential equation of slipping bond (Kuuskoski 1950, Rehm 1961), and time-consuming numerical integration of more complex bond-slip relationships can be omitted. The Tension Chord Model also allows, by equilibrium conditions only, determining steel strain

distributions between two adjacent cracks along a reinforcing bar – also referred to as crack element – with an almost arbitrary constitutive law (annex A), and hence, also to determine average steel strains in the crack element (annex B).

The bond stress level τ_{b1} is derived from theoretical considerations based on the local bond stress-slip law by Noakowski (1988); more details on the followed procedure are also provided in section 4.1 (see Zwicky 2013). The level τ_{b2} is calibrated from comparison of analytical calculations to experimental results of pull-out tests with long embedment lengths (Shima *et al.* 1987, Engström 1992). The following values of bond stress levels are proposed in conclusion (Sigrist 1995)

$$\tau_{b1} = 0.6 f_c^{2/3} \text{ and } \tau_{b2} = 0.3 f_c^{2/3} \quad (4)$$

where f_c = concrete cylinder compressive strength. These values correspond to $\tau_{b1} = 2f_{ctm}$ and $\tau_{b2} = f_{ctm} = 0.3(f_{ck})^{2/3}$, respectively, where f_{ctm} is the average concrete tensile strength (Model Code 2010, Model Code 1978). Note that the values of Eq. (4) are implicitly coupled to requirements on concrete cover thickness, bar ribbing and bar spacing.

2.4 Ductility properties of mild steel reinforcement

The behavior of the reinforcing steel in the post-yield domain, i.e., its hardening behavior and ductility properties, strongly affects the plastic deformation capacity of structural concrete (Alvarez 1998, Eligehausen and Mayer 2000, fib 2000, Mayer 2003). The ductility properties of reinforcing steel are generally described by the hardening ratio f_t/f_s and the ultimate strain ε_{su} (Model Code 2010). SIA 269/2 (2011) provides ductility classifications of older reinforcing steels used in Switzerland according to the classes of SIA 262 (2003) being the same as in Model Code (2010)

- Class A: $(f_t/f_s)_k \geq 1.05$ and $\varepsilon_{uk} \geq 25\%$
- Class B: $(f_t/f_s)_k \geq 1.05$ and $\varepsilon_{uk} \geq 25\%$
- Class C: $(f_t/f_s)_k \geq 1.15$ and $\varepsilon_{uk} \geq 75\%$

where f_{tk} = tensile strength; f_{sk} = yield strength and ε_{uk} = ultimate strain, all as characteristic values, i.e., 5th percentile. Note that the ultimate strain ε_{uk} is often governing for determining the ductility class of older (Swiss) reinforcing steel, not the hardening ratio $(f_t/f_s)_k$.

2.4.1 Impact of hardening behavior on strain localization and plastic deformation capacity

Fig. 2 shows examples of modeling the mechanical behavior of reinforcing steel of ductility class B with a typical yield strength of $f_{sk} = 500$ MPa, and in particular, the different models for capturing the hardening behavior, i.e., hot-rolled steel, cold-worked steel or a linear approximation. The associated analytical expressions are given in annex A.

For all hardening behaviors, a ratio of $(f_t/f_s)_k = 1.1$ is assumed. Onset of hardening of the hot-rolled steel shall take place at $\varepsilon_{sh} = 15\%$. The nominal yield strength of cold-worked steel is defined at a residual strain $\varepsilon_{s,pl} = 2\%$ and the proportional limit at a residual strain $\varepsilon_{s,pl} = 0.1\%$ (Section 2.2.3).

Fig. 3(a) shows strain localization factors $\kappa_s = \varepsilon_{sm} / \varepsilon_{smax}$ for steel strains ε_{smax} at cracks starting at ca. 2‰, associated with the different hardening behaviors of Fig. 2 and ε_{sm} according to the Tension Chord Model (annex B). The applied geometrical and mechanical parameters (bar diameter \varnothing , relative rib area f_R , concrete cover thickness c , bar spacing s , concrete compressive

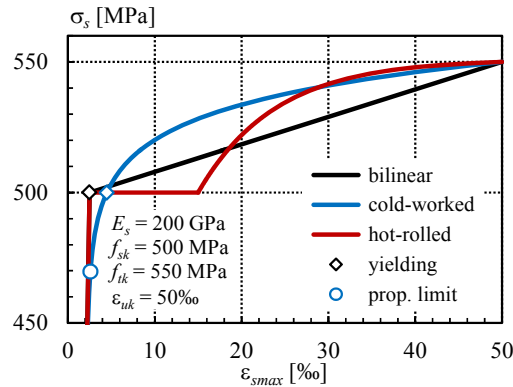


Fig. 2 Models for mechanical behavior of steel

strength f_{ck} and average crack spacing s_{rm}) serve as reference values for the further investigations, representing typical values encountered in existing structural elements which satisfy the requirements of new structures with regard to construction details (SIA 262 2003), also see Zwicky (2013).

The strain localization factors or tension stiffening, respectively, at and after the onset of yielding strongly depend on the hardening behavior (Section 2.2.2). Note that the principal form of the analytical graphs agrees well with experimental results (Alvarez and Marti 1996, Mayer and Eligehausen 1998, Eligehausen and Mayer 2000).

The main impact on the form of the graphs can be attributed to the changes in stiffness distribution along the reinforcing bar. The pronounced reduction after onset of yielding for hot-rolled and bilinearly approximated steel behavior is caused by the continuous extension of the length from the crack with plastic steel strains while the rest of the bar remains elastic. Pronounced localization of strains at the cracks is the consequence, and thus, small strain localization factors result. Once steel hardening at the crack is activated, the stiffness distribution becomes more equal and subsequently, strain localization factors reincrease. Once the strains in the whole crack element are beyond onset of hardening, the stiffness continuously decreases again. Consequently,

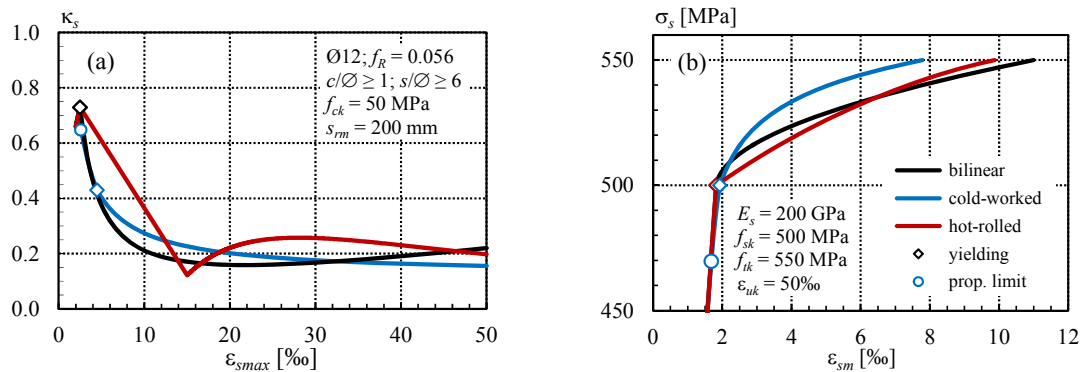


Fig. 3 Impact of reinforcing steel hardening behavior (a) on strain localization at cracks and (b) on average strains in a crack element with the mechanical behaviors of Fig. 2

the strain localization factors decrease again. The latter is not the case for bilinear modeling of steel behavior.

Analogous considerations apply to cold-worked steel behavior where the stiffness digressively decreases for strains beyond the proportional limit, being combined with the extension of plastified length as well. Consequently, the strain localization factors decrease digressively.

For the evaluation of maximum plastic deformation capacity $\Delta\varepsilon_{pl}$, the strain localization factors κ_{sy} at yielding and κ_{su} at ultimate are of major interest, Eq. (1). Table 1 summarizes the results, drawn from Fig. 3(a), for the strain localization factors at yielding as well as at attaining the proportional limit ε_{sp} of cold-worked steel, and at attaining the ultimate steel strain.

Multiplying the strain localization factors with the associated steel strains at cracks allows determining the total plastic deformation capacity of the tension chord element $\Delta\varepsilon_{pl} = \varepsilon_{smu} - \varepsilon_{smv} = \kappa_{su}\varepsilon_{uk} - \kappa_{sy}\varepsilon_{sv}$, also reported in Table 1. If reference is made to the proportional limit for cold-worked steel, a plastic deformation capacity increase of less than 5% is found. The values in Table 1 serve as references for the further evaluations.

Fig. 3(b) shows the deformation behavior of a crack element in terms of average steel strains ε_{sm} for the mechanical reinforcing steel behaviors from Fig. 2, i.e., the multiplication of the strain localization factors κ_s of Fig. 3(a) with the associated steel strains ε_{smax} at cracks. It can be easily deduced that a linear approximation of the hardening behavior generally tends to overestimate the plastic deformation capacity. Consequently, only the models of hot-rolled and cold-worked steel are used in the following evaluations for a more realistic assessment of plastic deformation capacity.

Cold-worked steel with the same ultimate strain as hot-rolled reinforcement provides less plastic deformation capacity, e.g. -27% for the chosen parameters, Table 1. Note that the reduced plastic deformation capacity of cold-worked steel is only secondarily related to the definition of the yield strength (Section 2.2.3). If reference is made to the proportional limit, the reduction in plastic deformation capacity still amounts to 24%.

2.4.2 Impact of ultimate strain on strain localization and plastic deformation capacity

It can naturally be expected that the ultimate strain ε_{uk} of the reinforcement has a crucial impact on plastic deformation capacity since it limits the maximum steel strain at cracks. Ultimate strains may vary largely in existing structures – to the favorable and to the unfavorable – in comparison to the requirements for more recent reinforcing steel.

Fig. 4 shows the impact of ultimate strain on average steel strains in a crack element. Table 2 summarizes the results for strain localization factors and plastic deformation capacity, the latter being also compared to the reference case (Fig. 3 and Table 1). Column labels “HR” refer to hot-rolled steel, labels “ CW_v ” to the yield limit and “ CW_p ” to the proportional limit of cold-worked steel, respectively. The proportional limit of cold-worked steel slightly varies due the applied

Table 1 Reference values of strain localization factors and plastic deformation capacity

Steel behavior		κ_{sy}	κ_{su}	$\Delta\varepsilon_{pl}$
Bilinear		0.73	0.22	9.16‰
Hot-rolled		0.73	0.20	8.03‰
Cold-worked	ε_{sv}	0.43	0.16	5.84‰
	ε_{sp}	0.65		6.09‰

Table 2 Impact of ultimate steel strain ε_{uk} on strain localization factors and plastic deformation capacity

ε_{uk}	25‰			50‰			75‰			100‰			125‰			
	Steel	HR	CW _y	CW _p	HR	CW _y	CW _p	HR	CW _y	CW _p	HR	CW _y	CW _p	HR	CW _y	CW _p
κ_{su}	0.73	0.44	0.64	0.73	0.43	0.65	0.73	0.43	0.65	0.73	0.43	0.66	0.73	0.42	0.66	
κ_{su}	0.31	0.22	0.20	0.16	0.16	0.13	0.14	0.12	0.13	0.11						
$\Delta\varepsilon_{pl}$	‰	5.88	3.61	3.91	8.03	5.84	6.09	10.19	7.84	8.06	12.34	9.72	9.92	14.50	11.51	11.71
	Rel.	73%	62%	64%	100%	127%	134%	132%	154%	166%	163%	181%	197%	192%		

analytical model, Eq. (7).

The impact of ultimate strain on the total plastic deformation capacity is linear for hot-rolled steel, and slightly less than proportional for cold-worked steel. More important, however, is the conclusion that a doubled or halved ultimate strain does not double or halve the plastic deformation capacity. From Fig. 4(b), it further becomes clear that it may be difficult to identify steel yielding from the global behavior of a tension chord reinforced with cold-worked steel, due to the continuity of the curves. This is related to the circumstance that cold-worked steel does not exhibit a sharp kink at attaining yielding but the constitutive law is continuous (Fig. 2). The reinforcing steel in the crack element must thus undergo a certain plastification before the global deformation behavior also shows observable stiffness decrease.

Cold-worked steel reaches between 61% and 79% of the plastic deformation capacity of hot-rolled steel with the same ultimate strain. Slightly higher values, varying between 67% and 81%, are found if the proportional limit is considered for onset of plastic strains. The unfavorable impact of cold-worked steel hardening behavior is thus partly compensated with increasing ultimate strain. This is related to the fact that strain localization factors for cold-worked steel essentially follow the same curve, Fig. 3(a), almost independently of the ultimate strain, and are thus somewhat higher for lower ultimate strains (Eligehausen *et al.* 1998, Zwicky 2012).

For the evaluation of plastic deformation capacity it is thus essential to know the value of ultimate strain as well as the fabrication process of the reinforcing steel. If first estimations reveal that the available ductility may limit the ultimate load of an existing structure (Section 1), gaining and testing specimens of reinforcing steel may therefore be advisable.

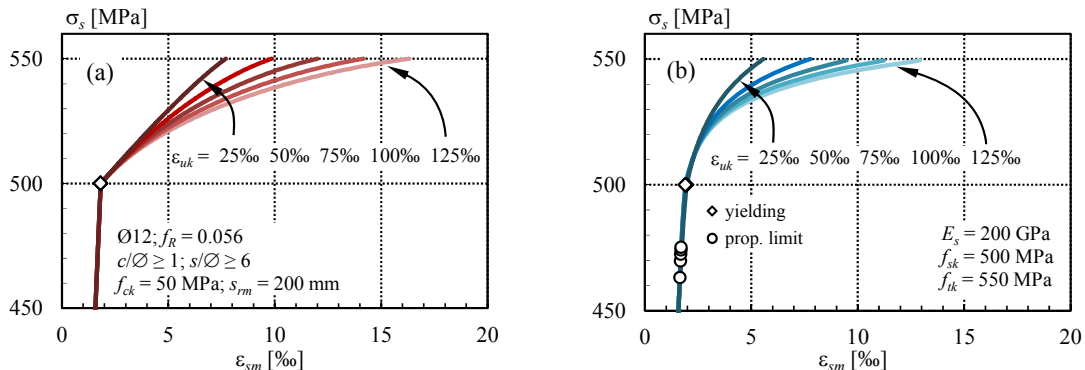


Fig. 4 Impact of ultimate strain ε_{uk} on average strains in a crack element for (a) hot-rolled and (b) cold-worked steel

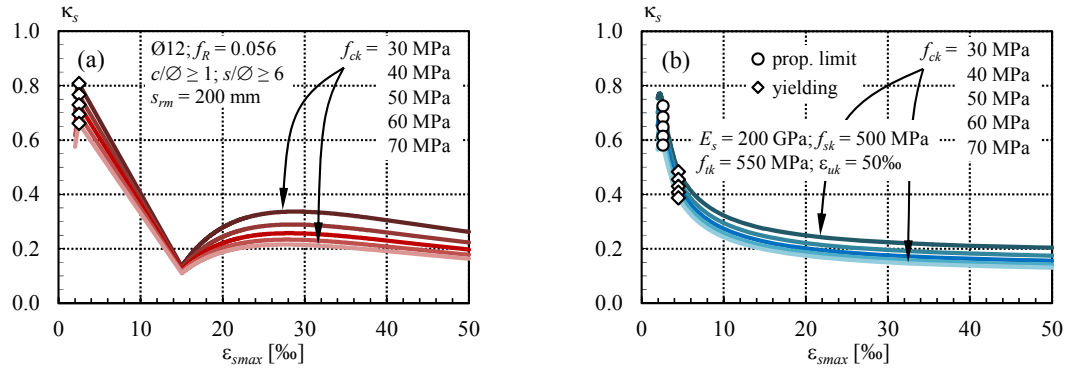


Fig. 5 Impact of concrete quality f_{ck} on strain localization for (a) hot-rolled and (b) cold-worked steel

2.5 Impact of concrete quality on strain localization and plastic deformation capacity

The quality of concrete – in particular around the reinforcing bars – has an immediate impact on bond strength, Eq. (4), and thus, on strain localization. In existing structures, concrete strength f_{ck} may vary considerably, from allegedly rather poor for structures from the very beginning of concrete construction history to rather strong for more recent structures, and in particular, prestressed and/or prefabricated structural elements. Note that concrete strength in the tension zone may be reduced due to fatigue loading (Sawko and Saha 1968). Concrete strength may also noticeably increase over the years due to hydration after the usual reference period of 28 days. Also, the concrete quality executed in practice may have been higher than what was prescribed in the project. Higher concrete strength usually is associated with a higher concrete rupture strain (Model Code 2010), thereby increasing the available plastic rotation capacity in plastic hinges if concrete crushing is governing, Eq. (2).

Fig. 5 shows the impact of concrete strength on strain localization factors in a crack element, determined on the basis of the Tension Chord Model (annex B). It can be seen that the precise value of concrete strength applied in the plastic deformation capacity assessment has a less pronounced impact than what would be expected. Comparable conclusions are found in Eligehausen *et al.* (1998) where numerical modeling (Kreller 1989) is applied for the determination of strain localization factors and average steel strains, based on a local bond stress-slip relationship (Eligehausen *et al.* 1983).

Table 3 Impact of concrete strength f_{ck} on strain localization factors and plastic deformation capacity

f_{ck}	30 MPa			40 MPa			50 MPa			60 MPa			70 MPa			
	Steel	HR	CW_y	CW_p	HR	CW_y	CW_p	HR	CW_y	CW_p	HR	CW_y	CW_p	HR	CW_y	CW_p
κ_{sy}	0.81	0.48	0.72	0.77	0.45	0.68	0.73	0.43	0.65	0.69	0.41	0.61	0.66	0.39	0.58	
κ_{su}	0.26	0.20	0.22	0.17	0.20	0.16	0.18	0.14	0.16	0.13						
$\Delta\epsilon_{pl}$	%	11.09	8.01	8.29	9.24	6.70	6.96	8.03	5.84	6.09	7.17	5.23	5.47	6.52	4.77	4.99
	Rel.	138%	137%	136%	115%	115%	114%	100%	89%	90%	90%	90%	81%	82%	82%	

Table 3 summarizes the results for strain localization factors and maximum plastic deformation capacities, also in comparison to the reference case (Section 2.4.1). It becomes obvious that the plastic deformation capacity is essentially independent of the hardening behavior of the reinforcing steel and of the referred value for the onset of plastic strains in cold-worked steel (Section 2.2.3). Cold-worked steel consistently attains 73% of the plastic deformation capacity of hot-rolled steel.

The plastic deformation capacity decreases with increasing concrete strength. However, since concrete strength in existing structures often attains rather high values of 50 MPa or more, its exact value matters less. For determining other essential structural characteristics such as shear or bending resistances, concrete strength has a considerable impact, of course.

3. Conclusions

This study is continued in Zwicky (2013), evaluating the impacts of construction and further structure-specific details on bond strength, strain localization and plastic deformation capacity.

References

- Alvarez, M. (1998), *Einfluss des Verbundverhaltens auf das Verformungsvermögen von Stahlbeton* (Influence of bond behavior on the deformation capacity of structural concrete, in German), **236**, Institute of Structural Engineering, Swiss Federal Institute of Technology, Zurich, Switzerland.
- Alvarez, M. and Marti, P. (1996), *Versuche zum Verbundverhalten von Bewehrungsstahl bei plastischen Verformungen* (Tests on the bond behavior of reinforcing steel exposed to plastic deformations, in German), **222**, Institute of Structural Engineering, Swiss Federal Institute of Technology, Zurich, Switzerland.
- Bachmann, H. (1967), *Zur Plastizitätstheoretischen Berechnung statisch unbestimmter Stahlbetonbalken* (On the plasticity-based analysis of statically indeterminate reinforced concrete girders, in German), **13**, Institute of Structural Engineering, Swiss Federal Institute of Technology, Zurich, Switzerland.
- Brühwiler, E., Vogel, T., Lang, T. and Lüchinger, P. (2012), "Swiss standards for existing structures", *Struct. Eng. Int.*, **22**(2), 275-280.
- Burns, C. (2011), *Serviceability analysis of reinforced concrete based on the tension chord model*, PhD thesis no. 19979, Institute of Structural Engineering, Swiss Federal Institute of Technology, Zurich, Switzerland.
- Cosenza, E., Greco, C. and Manfredi, G. (1993), *The concept of equivalent steel*, Progress Report of Task Group 2.2 'Ductility Requirements for Structural Concrete – Reinforcement, Bulletin d'Information no. 218, Comité Euro-International du Béton (CEB), Lausanne, Switzerland, 163-183.
- Eligehausen, R., Popov, E.P. and Bertero, V.V. (1983), *Local bond stress-slip relationships of deformed bars under generalized excitations*, **UCB/EERC 83/23**, Earthquake Engineering Research Center, University of California, Berkeley CA, USA.
- Eligehausen, R., Ozbolt, J. and Mayer, U. (1998), *Contribution of concrete between cracks at inelastic steel strains and conclusions for the optimization of bond*, Leon, R. (ed.), *Bond and Development of Reinforcement: a tribute to Dr. Peter Gergely*, ACI-International SP-180, 45-80.
- Eligehausen, R. and Mayer, U. (2000), *Untersuchungen zum Einfluss der bezogenen Rippenfläche von Bewehrungsstäben auf das Tragverhalten von Stahlbetonbauteilen im Gebrauchs- und Bruchzustand* (Investigations on the influence of the relative rib area of reinforcing bars on the structural behavior of reinforced concrete members in the serviceability and ultimate limit state, in German), **503**, Deutscher Ausschuss für Stahlbeton, Beuth Berlin, Germany.

- Engström, B. (1992), *Ductility of tie connections in precast structures*, publ. no. 92:1, Division of Concrete Structures, Dept. of Structural Engineering, Chalmers University of Technology, Gothenburg, Sweden.
- fib (2000), *Bond mechanisms including pull-out and splitting failures*, Bond of reinforcement in concrete – state-of-the-art report, bulletin no. 10, International Federation for Structural Concrete (fib), Lausanne, Switzerland, 1-98.
- Kaufmann, W. and Marti, P. (1998), “Structural concrete: Cracked membrane model”, *ASCE J. Struct. Eng.*, **124**(12), 1467-1475.
- Kaufmann, W. (1998), *Strength and deformations of structural concrete subjected to in-plane shear and normal forces*, **234**, Institute of Structural Engineering, Swiss Federal Institute of Technology, Zurich, Switzerland.
- Kenel, A. (2002), *Biegetragverhalten und Mindestbewehrung von Stahlbetonbauteilen* (Bending behavior and minimum reinforcement of structural concrete elements, in German), **277**, Institute of Structural Engineering, Swiss Federal Institute of Technology, Zurich, Switzerland.
- Kreller, H. (1989), *Zum nichtlinearen Verformungsverhalten von Stahlbetontragwerken unter Last- und Zwangeinwirkung* (On the non-linear behavior of reinforced concrete structures under load and restraint actions, in German), **1989/4**, Institute of Construction Materials, University of Stuttgart, Germany.
- Kuuskoski, V. (1950), *Über die Haftung zwischen Beton und Stahl* (On the adherence between concrete and steel, in German), **19**, Technische Hochschule von Finland (The State Institute for Technical Research), Helsinki, Finland.
- Marti, P., Sigrist, V. and Alvarez, M. (1997), *Mindestbewehrung von Betonbauten* (Minimum reinforcement of concrete structures, in German), **529**, Swiss Federal Highway Administration, Berne, Switzerland.
- Marti, P., Alvarez, M., Kaufmann, W. and Sigrist, V. (1998), “Tension chord model for structural concrete”, *Struct. Eng. Int.*, **8**(4), 287-298.
- Mayer, U. and Eligehausen, R. (1998), “Bond behavior of ribbed bars at inelastic steel strains”, *Proc. 2nd Int'l PhD Symp. in Civil Eng.*, Technical University of Budapest, Hungary, 39-46.
- Mayer, U. (2003), *Zum Einfluss der Oberflächengestalt von Rippenstählen auf das Trag- und Verformungsverhalten von Stahlbetonbauteilen* (Influence of the rib pattern of ribbed reinforcement on the structural behavior of reinforced concrete members, in German), **537**, Deutscher Ausschuss für Stahlbeton, Beuth Berlin, Germany.
- Model Code (2010), *Model code 2010 – Final draft, Vol. 1*, **65**, International Federation for Structural Concrete (fib), Lausanne, Switzerland.
- Model Code (1978), *CEB-FIP Model code for concrete structures*, 3rd edition, Comité Euro-International du Béton, Paris, France.
- Nielsen, M.P. and Hoang, L.C. (2010), *Limit analysis and concrete plasticity*, 3rd edition, Taylor & Francis.
- Noakowski, P. (1988), *Nachweisverfahren für Verankerung, Verformung, Zwangsbeanspruchung und Rissbreite* (Verification procedure for anchorage, deformation, restraint loading and crack width, in German), **394**, Deutscher Ausschuss für Stahlbeton, Beuth Berlin, Germany.
- Rehm, G. (1961), *Über die Grundlagen des Verbunds zwischen Stahl und Beton* (On the fundamentals of bond between steel and concrete, in German), **138**, Deutscher Ausschuss für Stahlbeton, Ernst & Sohn Berlin, Germany.
- Sawko, F. and Saha, G.P. (1968), “Fatigue of concrete and its effect upon prestressed concrete beams”, *Mag. Concrete Res.*, **20**(62), 21-30.
- Shima, H., Chou, L.L. and Okamura, H. (1987), “Micro and macro models for bond in reinforced concrete”, *J. Faculty Eng.*, **39**(2), 133-194.
- SIA 262 (2003), *Concrete structures*, Swiss Society of Engineers and Architects (SIA), Zurich, Switzerland.
- SIA 269/2 (2011), *Existing structures – concrete structures*, Swiss Society of Engineers and Architects (SIA), Zurich, Switzerland (currently only available in German and French).
- Sigrist, V. (1995), *Zum Verformungsvermögen von Stahlbetonträgern* (On the deformation capacity of reinforced concrete girders, in German), **210**, Institute of Structural Engineering, Swiss Federal Institute of Technology, Zurich, Switzerland.
- Sigrist, V. and Marti, P. (1994), “Ductility of structural concrete: A contribution”, *Proc. Workshop*

- Development of EN 1992 in Relation to New Research Results and to the CEB-FIP Model Code 1990*, Czech Technical University, Prague, Czech Republic, 211-223.
- Zwicky, D. (2013), "Bond and ductility: a theoretical study on the impact of construction details – part 2: structure-specific features", *Adv. Concrete Constr.*, **1**(2).
- Zwicky, D. (2012), "Effects of construction details in existing concrete structures on bond", *Proc. Bond in Concrete 'Bond, Anchorage, Detailing'*, 4th Int'l Symp., Brescia, Italy, 23-30.

Appendix A. Analytical models for mechanical behavior of reinforcing steel

- Bilinear approximation (i.e. linear hardening)

$$(5) \quad \sigma_s = E_s \varepsilon_s \quad \text{for } 0 \leq \varepsilon_s \leq \varepsilon_{sy}$$

$$(6) \quad \sigma_s = f_{sy} + E_{sh} (\varepsilon_s - \varepsilon_{sy}) \quad \text{for } \varepsilon_{sy} < \varepsilon_s \leq \varepsilon_{su}$$

- Cold-worked steel (Cosenza *et al.* 1993)

$$(7) \quad \varepsilon_s = \frac{\sigma_s}{E_s} + \left(\frac{\sigma_s}{k_y} \right)^\alpha \quad \text{with } \alpha = \frac{\ln \left[(\varepsilon_{su} - f_{su}/E_s) / \varepsilon_{s,pl} \right]}{\ln (f_{su}/f_{sy})} \quad \text{and } k_y = \frac{f_{sy}}{\varepsilon_{s,pl}^{1/\alpha}}$$

Note that Eq. (7) cannot be inverted to express σ_s as a function of ε_s .

- Hot-rolled steel (Cosenza *et al.* 1993)

$$(8) \quad \sigma_s = E_s \varepsilon_s \quad \text{for } 0 \leq \varepsilon_s \leq \varepsilon_{sy}$$

$$(9) \quad \sigma_s = f_{sy} \quad \text{for } \varepsilon_{sy} < \varepsilon_s \leq \varepsilon_{sh}$$

$$(10) \quad \sigma_s = f_{sy} + (f_{su} - f_{sy}) k_c \left[1 - e^{(\varepsilon_{sh} - \varepsilon_s)/\beta} \right] \quad \text{with } \beta = k_a \frac{\varepsilon_{sh} - \varepsilon_{su}}{\varepsilon_{sh} - k_b} \quad \text{for } \varepsilon_{sh} < \varepsilon_s \leq \varepsilon_{su}$$

The parameters k_a , k_b and k_c shall be chosen such that they fit closely the experimentally measured hardening behavior and that they furthermore fulfill the requirement

$$(11) \quad \varepsilon_{sh} = k_b + k_a \ln \left(\frac{k_c - 1}{k_c} \right).$$

In the present study, $k_a = 0.0245$ and $k_c = 1.019858734$ is adopted (Alvarez 1998) and k_b is determined from Eq. (11) as a function of the chosen ε_{sh} .

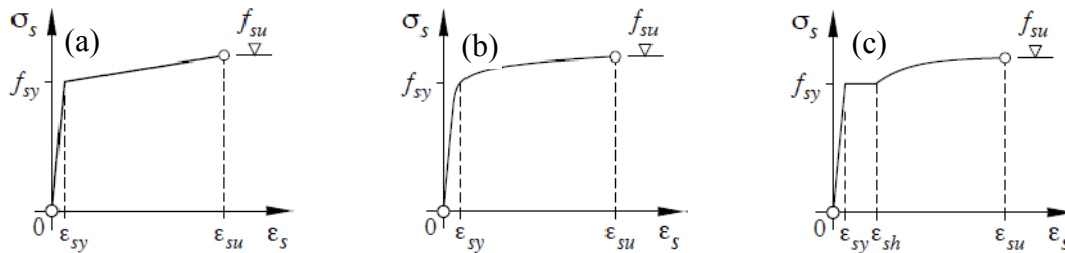


Fig. A.1 Constitutive law models for reinforcing steel (Alvarez 1998) – (a) bilinear approximation, (b) cold-worked steel and (c) hot-rolled steel

Appendix B. Average steel strains in a tension chord

The average steel strains ε_{sm} in a tension chord with an average crack spacing s_{rm} , a reinforcing bar of diameter \varnothing , and a given hardening behavior can be determined from the following expressions (Alvarez 1998), according to the Tension Chord Model (Sigrist 1995, Marti *et al.* 1998), Fig. 1.

- Steel with linear hardening

$$(12) \quad \varepsilon_{sm} = \frac{\sigma_{smax} - \tau_{b1}s_{rm}}{E_s} \quad \text{for } \sigma_{smax} \leq f_{sy}$$

$$(13) \quad \varepsilon_{sm} = \frac{(\sigma_{smax} - f_{sy})^2 \varnothing}{4E_{sh}\tau_{b2}s_{rm}} \left(1 - \frac{E_{sh}\tau_{b1}}{E_s\tau_{b2}}\right) + \frac{(\sigma_{smax} - f_{sy})\tau_{b1}}{E_s\tau_{b2}} + \left(\varepsilon_{sy} - \frac{\tau_{b1}s_{rm}}{E_s\varnothing}\right)$$

for $f_{sy} \leq \sigma_{smax} \leq f_{sy} + 2\tau_{b2} \frac{s_{rm}}{\varnothing}$

$$(14) \quad \varepsilon_{sm} = \frac{\sigma_{smax} - f_{sy}}{E_{sh}} + \left(\varepsilon_{sy} - \frac{\tau_{b2}s_{rm}}{E_{sh}\varnothing}\right) \quad \text{for } f_{sy} + 2\tau_{b2} \frac{s_{rm}}{\varnothing} \leq \sigma_{smax} \leq f_{su}$$

- Cold-worked steel

$$(15) \quad \varepsilon_{sm} = \frac{\sigma_{smax} - \tau_{b1}s_{rm}}{E_s} + \frac{\varnothing}{2\tau_{b1}s_{rm}} \frac{1}{(1+\alpha)k_y^\alpha} \left[\sigma_{smax}^{1+\alpha} - \left(\sigma_{smax} - 2\tau_{b1} \frac{s_{rm}}{\varnothing} \right)^{1+\alpha} \right]$$

for $0 \leq \sigma_{smax} \leq f_{sy}$

$$(16) \quad \varepsilon_{sm} = \frac{\varnothing}{4E_s\tau_{b2}s_{rm}} \left\{ \begin{array}{l} \left(\sigma_{smax} - f_{sy} \right)^2 \left(1 - \frac{\tau_{b1}}{\tau_{b2}} \right) \\ + \frac{2E_s}{(1+\alpha)k_y^\alpha} \left[\sigma_{smax}^{1+\alpha} - f_{sy}^{1+\alpha} \left(1 - \frac{\tau_{b2}}{\tau_{b1}} \right) - \right. \\ \left. \frac{\tau_{b2}}{\tau_{b1}} \left(f_{sy} + \frac{\tau_{b1}}{\tau_{b2}} (\sigma_{smax} - f_{sy}) - 2\tau_{b1} \frac{s_{rm}}{\varnothing} \right)^{1+\alpha} \right] \end{array} \right\}$$

$$+ \frac{\tau_{b1}}{\tau_{b2}} \left[\frac{\sigma_{smax}}{E_s} - \frac{f_{sy}}{E_s} \left(1 - \frac{\tau_{b2}}{\tau_{b1}} \right) \right] - \frac{\tau_{b1}s_{rm}}{E_s\varnothing}$$

for $f_{sy} \leq \sigma_{smax} \leq f_{sy} + 2\tau_{b2} \frac{s_{rm}}{\varnothing}$

$$(17) \quad \varepsilon_{sm} = \frac{\sigma_{smax}}{E_s} - \frac{\tau_{b2} s_{rm}}{E_s \emptyset} + \frac{\emptyset}{2\tau_{b2} s_{rm}} \frac{1}{(1+\alpha) k_y^\alpha} \left[\sigma_{smax}^{1+\alpha} - \left(\sigma_{smax} - 2\tau_{b2} \frac{s_{rm}}{\emptyset} \right)^{1+\alpha} \right]$$

for $f_{sy} + 2\tau_{b2} \frac{s_{rm}}{\emptyset} \leq \sigma_{smax} \leq f_{su}$

- Hot-rolled steel

$$(18) \quad \varepsilon_{sm} = \frac{\sigma_{smax}}{E_s} - \frac{\tau_{b1} s_{rm}}{E_s \emptyset} \quad \text{for } 0 \leq \sigma_{smax} \leq f_{sy}$$

$$(19) \quad \varepsilon_{sm} = \frac{\emptyset}{2\tau_{b2} s_{rm}} \left[\varepsilon_{sh} (\sigma_{smax} - f_{sy}) + k_c (f_{su} - f_{sy}) \beta \{1 + z_1 [\ln(z_1) - 1]\} \right] + \frac{s_{rm} - 2\tilde{x}}{s_{rm}} \left[\varepsilon_{sy} - \frac{\tau_{b1} (s_{rm} - 2\tilde{x})}{E_s \emptyset} \right]$$

for $f_{sy} \leq \sigma_{smax} \leq f_{sy} + 2\tau_{b2} \frac{s_{rm}}{\emptyset}$

$$(20) \quad \varepsilon_{sm} = \varepsilon_{sh} - \frac{\emptyset}{2\tau_{b2} s_{rm}} k_c (f_{su} - f_{sy}) \beta \{z_2 [\ln(z_2) - 1] - z_1 [\ln(z_1) - 1]\}$$

for $f_{sy} + 2\tau_{b2} \frac{s_{rm}}{\emptyset} \leq \sigma_{smax} \leq f_{su}$

with the auxiliary parameters

$$(21) \quad \tilde{x} = \frac{(\sigma_{smax} - f_{sy}) \emptyset}{4\tau_{b2}}, \quad z_1 = 1 - \frac{\sigma_{smax} - f_{sy}}{k_c (f_{su} - f_{sy})} \quad \text{and} \quad z_2 = 1 - \frac{\sigma_{smax} - f_{sy} - 2\tau_{b2} s_{rm} / \emptyset}{k_c (f_{su} - f_{sy})}.$$

Notations

A_c	gross concrete cross-section
A_s	cross-section of longitudinal reinforcement
C	bond-slip law parameter
E_s	Young's modulus of reinforcing steel
E_{sh}	hardening modulus of reinforcing steel
N	bond-slip law parameter
b	width of concrete compression zone
c	concrete cover thickness
c_{lat}	lateral concrete cover thickness
d	effective depth of reinforcement
f_c	concrete cylinder compressive strength
f_{ck}	characteristic value of concrete cylinder compressive strength
f_{ctm}	average concrete tensile strength
f_{cu}	uniaxial concrete compressive strength
f_R	relative rib area

f_{sk}	characteristic value of yield strength of reinforcing steel
f_{su}	nominal ultimate strength of reinforcing steel
f_{sy}	nominal yield strength of reinforcing steel
f_{tk}	characteristic value of tensile strength of reinforcing steel
k_a	form parameter for constitutive law of hot-rolled steel
k_b	form parameter for constitutive law of hot-rolled steel
$k_{b,c}$	bond strength reduction factor related to concrete cover thickness
$k_{b,c,lat}$	bond strength reduction factor related to interaction of orthogonal concrete covers
$k_{b,fR}$	bond strength reduction factor related to relative rib area
$k_{b,s}$	bond strength reduction factor related to reduced bar spacing
k_c	form parameter for constitutive law of hot-rolled steel
k_y	parameter related to nominal yielding of cold-worked steel
s	bar spacing
s_{crit}	critical bar spacing
s_{rm}	average crack spacing
x	plastic height of compression zone
θ_{pl}	maximum plastic rotation angle
$\Delta\varepsilon_{pl}$	total plastic strain capacity
α	form parameter for constitutive law of cold-worked steel
β	form parameter for constitutive law of hot-rolled steel
γ	failure cone inclination
ε_{cnu}	nominal concrete crushing strain
ε_s	steel strain
ε_{sha}	steel strain at onset of hardening of hot-rolled steel
ε_{sm}	average steel strain between two adjacent cracks
ε_{smax}	maximum steel strain at cracks
ε_{smu}	average steel strain at attaining ultimate
ε_{smy}	average steel strain at attaining yielding
ε_{sp}	proportional limit strain of reinforcing steel
$\varepsilon_{s,pl}$	residual strain of reinforcing steel
ε_{su}	nominal ultimate strain of reinforcing steel
ε_{sy}	yield strain of reinforcing steel
ε_{uk}	characteristic value of ultimate strain of reinforcing steel
κ_s	strain localization factor for steel
κ_{sy}	strain localization factor at yielding
κ_{su}	strain localization factor at ultimate
ρ	geometrical reinforcement ratio
σ_s	steel stress
σ_{smax}	steel stress at cracks
τ_{b1}	average bond stress before onset of yielding
τ_{b2}	average bond stress after onset of yielding
τ_{bm}	average bond stress on anchorage length
ω	mechanical reinforcement ratio
\emptyset	bar diameter